medRxiv preprint doi: https://doi.org/10.1101/2023.09.04.23295018; this version posted September 5, 2023. The copyright holder for this preprint (which was not certified by peer review) is the author/funder, who has granted medRxiv a license to display the preprint in perpetuity. All rights reserved. No reuse allowed without permission.

A powerful replicability analysis of genome-wide association studies

Yan Li[1], Haochen Lei[2], Xiaoquan Wen[3] and Hongyuan Cao[2*]

Abstract

Replicability is the cornerstone of modern scientific research. Reliable identifications of genotype-phenotype associations that are significant in multiple genome-wide association studies (GWASs) provide stronger evidence for the findings. Current replicability analysis relies on the independence assumption among single nucleotide polymorphisms (SNPs) and ignores the linkage disequilibrium (LD) structure. We show that such a strategy may produce either overly liberal or overly conservative results in practice. We develop an efficient method, ReAD, to detect replicable SNPs associated with the phenotype from two GWASs accounting for the LD structure. The local dependence structure of SNPs across two heterogeneous studies is captured by a four-state hidden Markov model (HMM) built on two sequences of p-values. By incorporating information from adjacent locations via the HMM, our approach provides more accurate SNP significance rankings. ReAD is scalable, platform independent and more powerful than existing replicability analysis methods with effective false discovery rate (FDR) control. Through analysis of datasets from two asthma GWASs and two ulcerative colitis

[1]School of Mathematics, Jilin University, Changchun, Jilin 130012, China.
[2]Department of Statistics, Florida State University, Tallahassee, FL 32306, USA.
[3]Department of Biostatistics, University of Michigan, Ann Arbor, MI 48109, USA.
[*]Corresponding author: hongyuancao@gmail.com

NOTE: This preprint reports new research that has not been certified by peer review and should not be used to guide clinical practice.

medRxiv preprint doi: https://doi.org/10.1101/2023.09.04.23295018; this version posted September 5, 2023. The copyright holder for this preprint (which was not certified by peer review) is the author/funder, who has granted medRxiv a license to display the preprint in perpetuity. All rights reserved. No reuse allowed without permission.

GWASs, we show that ReAD can identify replicable genetic loci that existing methods might otherwise miss.

1 Introduction

Genome-wide association studies (GWASs) allow for simultaneous study of millions of single nucleotide polymorphisms (SNPs). Numerous genetic risk variants associated with various phenotypes and complex diseases have been reported over the past couple of decades (McCarthy et al., 2008; MacArthur et al., 2017). These associations provide insights into the architecture of disease susceptibility. Despite these progresses, many reported genotype-phenotype associations fail to replicate in other studies (Ioannidis et al., 2001; Chanock et al., 2007). An analysis of past studies indicates that the cumulative prevalence of irreplicable preclinical research (including GWAS) exceeds 50% (Ioannidis, 2005; Prinz et al., 2011; Begley and Ellis, 2012; Freedman et al., 2015). Approximately 28 billion annually is spent on preclinical research that is not replicable in the United States alone (Freedman et al., 2015). Irreplicable and/or inconsistent between-study associations might be spurious findings caused by confounding factors, such as population stratification, misclassification of phenotypes, genotyping errors, or technical biases, among others. Replicability is now considered a *sine qua non* for establishing credible genotype-phenotype associations in the era of GWAS (Moonesinghe et al., 2008; Huffman, 2018). We study conceptual replicability where consistent results are obtained using different processes and populations that target the same scientific question. For GWASs, replicability analysis aims to detect genetic risk loci that are significantly associated with the same phenotype across different studies (Heller and Yekutieli, 2014; Heller et al., 2014; Bogomolov and Heller, 2022). By eliminating genetic associations that can not be generalized across studies, replicability analysis provides stronger support for genuine scientific findings, avoids wasted resources, and improves efficiency of drug development. This

medRxiv preprint doi: https://doi.org/10.1101/2023.09.04.23295018; this version posted September 5, 2023. The copyright holder for this preprint (which was not certified by peer review) is the author/funder, who has granted medRxiv a license to display the preprint in perpetuity. All rights reserved. No reuse allowed without permission.

helps the translation of bench discoveries to bedsided therapies.

In GWASs, millions of SNPs are tested simultaneously, requiring multiple testing adjustment. False discovery rate (FDR), defined as the expectation of the proportion of false discoveries over total discoveries, is a commonly used metric for type I error control (Benjamini and Hochberg, 1995). A central characteristic of GWAS data is the linkage disequilibrium (LD) among SNPs, with which alleles at nearby sites can co-occur on the same haplotype more often than by chance alone (Pritchard and Przeworski, 2001; Wall and Pritchard, 2003). As a result, it is common to observe that phenotype-associated SNPs form clusters and exhibit high correlations within clusters (Wei et al., 2009). An effective approach to account for the LD structure among SNPs is through the hidden Markov model (HMM) (Churchill, 1992). Existing GWAS literature (Sun and Cai, 2009; Wei et al., 2009) using HMM for a single study is not applicable to replicability analysis of multiple studies. Furthermore, their approaches cannot be generalized to more than one study due to the heterogeneity of LD across different studies (Lonjou et al., 2003). Replicability analysis of GWASs explicitly accounting for the LD structure has not been studied before to the best of our knowledge.

To claim replicability, an *ad hoc* approach is to implement an FDR control method, such as the Benjamini and Hochberg (BH) procedure (Benjamini and Hochberg, 1995), for each study and intersect significant results from all studies as replicable findings. This approach does not control the FDR and moreover has low power as it does not borrow information from different studies. The maximum of p-values across studies ($P_{\max}$) is a straightforward significance measure for replicability (Benjamini et al., 2009). After summarizing data from multiple studies by $P_{\max}$, classic FDR control procedures such as BH are used for replicability analysis. This procedure is overly conservative as it guards against the worst scenario and does not incorporate the composite null structure of replicability analysis. For independent features from high-throughput experiments, various methods were proposed for replicability analysis. These methods are not robust to heterogeneity of different studies (Li et al., 2011; Philtron

medRxiv preprint doi: https://doi.org/10.1101/2023.09.04.23295018; this version posted September 5, 2023. The copyright holder for this preprint (which was not certified by peer review) is the author/funder, who has granted medRxiv a license to display the preprint in perpetuity. All rights reserved. No reuse allowed without permission.

et al., 2018), require tuning parameters (Zhao et al., 2020), impose parametric assumptions on the p-values (Heller et al., 2014) or demand access to full datasets which can be prohibitive due to privacy concerns or logistics (McGuire et al., 2021).

We address the limitations of existing methods by developing an efficient method, ReAD (Replicability Analysis accounting for Dependence) to detect replicable genotype-phenotype associations across two GWASs by incorporating the LD structure. We use GWAS summary statistics such as p-values, treating multiple studies symmetrically. Our approach models the clustered signals from two studies with a four-dimensional HMM accounting for the heterogeneity of LD structures in different studies. Conditional on the HMM, we model the two p-value sequences as a four-group mixture of SNPs (Efron, 2012; Chung et al., 2014). The replicability null hypothesis consists of three components: zero effects in both studies, zero effect in one study and non-zero effect in another study and vice versa. ReAD calculates the posterior probability of replicability null given data. Compared to other replicability analysis methods, ReAD is robust as it is non-parametric, jointly models the signal and non-signal from different studies, and accounts for the heterogeneity of different studies. ReAD provides more efficient rankings of importance for replicable SNPs by pooling information from two p-value sequences via the forward and backward probabilities (Rabiner and Juang, 1986; Murphy, 2012). ReAD applies a step-up procedure to identify clusters of genotype-phenotype associated signals, improving the power of replicability analysis while effectively controlling the FDR. ReAD is computationally scalable to whole genome with tens of millions of SNPs. Its implementation combines the non-parametric expectation-maximization (EM) algorithm (Dempster et al., 1977) and the pool-adjacent-violator algorithm (PAVA) in shape constraint inference (Robertson et al., 1988; Busing, 2022), without any tuning parameters. We conduct extensive simulation studies to evaluate the performance of our approach across a wide range of scenarios. By applying our procedure to summary statistics of two asthma GWASs and two ulcerative colitis GWASs, we show that ReAD identifies more replicable genetic loci that

medRxiv preprint doi: https://doi.org/10.1101/2023.09.04.23295018; this version posted September 5, 2023. The copyright holder for this preprint (which was not certified by peer review) is the author/funder, who has granted medRxiv a license to display the preprint in perpetuity. All rights reserved. No reuse allowed without permission.

otherwise might be missed using existing methods that do not account for the LD structure. These identified association signals pinpoint potential new loci on metabolisms and immunity.

2 Results

2.1 Method overview

ReAD takes p-values from two independent GWASs with the same phenotype as input. Suppose we have J SNPs with corresponding p-values $(p_{1j}, p_{2j}), j = 1, \ldots, J$. We aim to identify replicable SNPs associated with the phenotype in both studies. Our method can handle SNPs in the whole genome where J is in the order of millions. We use θ_{ij} to represent the inferred association status of SNP j in study i. For each SNP, we consider its association analysis

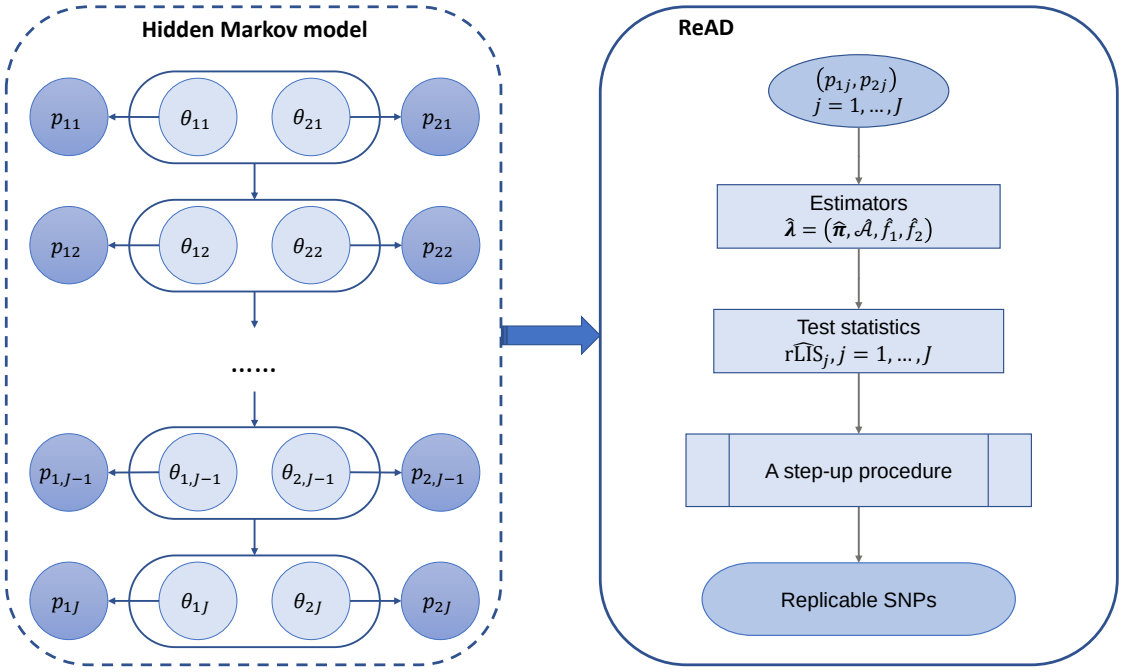

Figure 1: Schematic of ReAD. θ_{ij} represents the inferred association status of SNP j ($j = 1, \ldots, J$) in study i ($i = 1, 2$). For each SNP j, we consider its association analysis results are replicable if $\theta_{1j} = \theta_{2j} = 1$. The dependence structure among SNPs across two studies can be modeled with a HMM.

medRxiv preprint doi: https://doi.org/10.1101/2023.09.04.23295018; this version posted September 5, 2023. The copyright holder for this preprint (which was not certified by peer review) is the author/funder, who has granted medRxiv a license to display the preprint in perpetuity. All rights reserved. No reuse allowed without permission.

results are replicable if its corresponding θ values are consistently 1. The correlations between θ's within a study are caused by LD among tested SNPs, and we model their dependence structure using a Markov chain. Following Li and Stephens (2003), this is an effective way to model the correlations between observed p-values. Given the observed p-values are from both studies, the overall model structure can be represented by a HMM.

We present our schematic in Figure 1. We use $s_j \in \{0, 1, 2, 3\}$ to denote the joint inferred association status for SNP j, where $s_j = 0$ if $\theta_{1j} = \theta_{2j} = 0$, $s_j = 1$ if $\theta_{1j} = 0$ and $\theta_{2j} = 1$, $s_j = 2$ if $\theta_{1j} = 1$ and $\theta_{2j} = 0$, and $s_j = 3$ if $\theta_{1j} = \theta_{2j} = 1$. The composite null for replicability analysis corresponds to $s_j \in \{0, 1, 2\}$. To capture the local dependence of LD structure among SNPs, we impose a four-state HMM on $\boldsymbol{s} = (s_1, \ldots, s_J)$. The transition matrix is denoted as $\mathcal{A} = \{a_{kl} : k, l = 0, 1, 2, 3\}$, where the transition probability from $s_j = k$ to $s_{j+1} = l$ is given by a_{kl}, and $\sum_{l=0}^{3} a_{kl} = 1$ for all k. An efficient EM algorithm in combination with the forward-backward procedure and PAVA is developed to estimate the unknown parameters and functions. We use the posterior probability of being replicability null, $\text{rLIS}_j, j = 1, \ldots, J$, as the test statistic and obtain $\widehat{\text{rLIS}}_j$ for all SNPs. By applying a step-up procedure on $\widehat{\text{rLIS}}_j, j = 1, \ldots, J$, we get powerful testing results while controlling the FDR. More details of ReAD can be found in the Methods Section and the Supplemental Note A.

2.2 Simulation study

2.2.1 Simulation I

In simulation I, we evaluated the FDR and statistical power of ReAD based on the rLIS statistic across two studies. Here power is defined as the averaged proportion of true discoveries among the total number of non-null hypotheses. We compare the FDR and power of ReAD with several replicability analysis methods developed under independence, including the *ad hoc* BH method, the MaxP method based on $P_{\max}$(Benjamini et al., 2009) and the STAREG

medRxiv preprint doi: https://doi.org/10.1101/2023.09.04.23295018; this version posted September 5, 2023. The copyright holder for this preprint (which was not certified by peer review) is the author/funder, who has granted medRxiv a license to display the preprint in perpetuity. All rights reserved. No reuse allowed without permission.

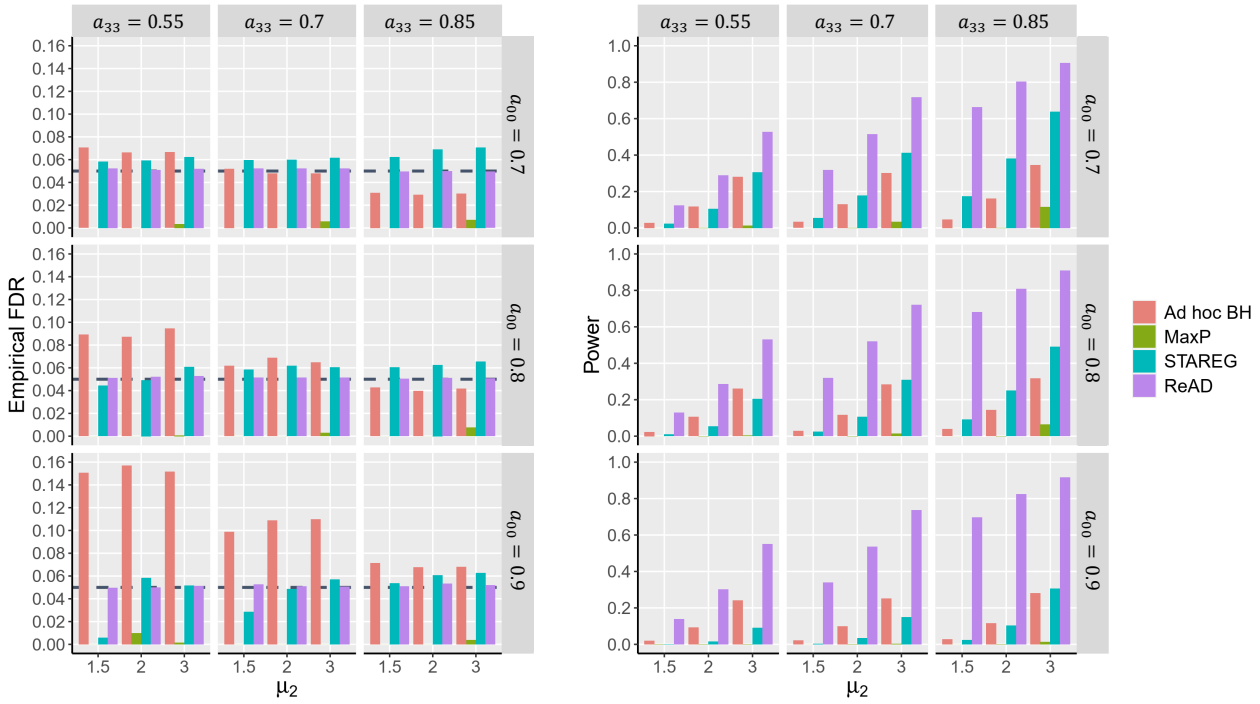

Figure 2: FDR control and power comparison of different methods.

method based on the local false discovery rate (Lfdr) (Li et al., 2023). Details of these methods can be found in the Supplemental Note B. An extensive comparison with more replicability analysis methods can be found in Supplemental Note C.

In each simulation, the hidden states of $10,000$ SNPs were generated from a four-state Markov chain. A detailed description of the data generating process is provided in Supplemental Note C. In all simulations, we fix the initial distribution of four states as $\boldsymbol{\pi} = (0.9, 0.025, 0.025, 0.05)$. The signals from two studies are generated from normal distributions with mean μ_i and variance $\sigma_i^2, i = 1, 2$. We vary the transition matrix $\mathcal{A} = \{a_{kl} : k, l = 0, 1, 2, 3\}$ and μ_2 while fix $\mu_1 = 2$, and $\sigma_1 = \sigma_2 = 1$. Empirical FDR and power are calculated from 100 replications for each setting. The results are summarized in Figure 2 (left: FDR; right: power). In Figure 2, each row corresponds to a different a_{00}, and each column corresponds to a different a_{33}. In each panel, we set μ_2 to $1.5, 2$, or 3. At FDR level 0.05, we see that the *ad hoc* BH fails to control the FDR. MaxP is overly conservative across all settings.

medRxiv preprint doi: https://doi.org/10.1101/2023.09.04.23295018; this version posted September 5, 2023. The copyright holder for this preprint (which was not certified by peer review) is the author/funder, who has granted medRxiv a license to display the preprint in perpetuity. All rights reserved. No reuse allowed without permission.

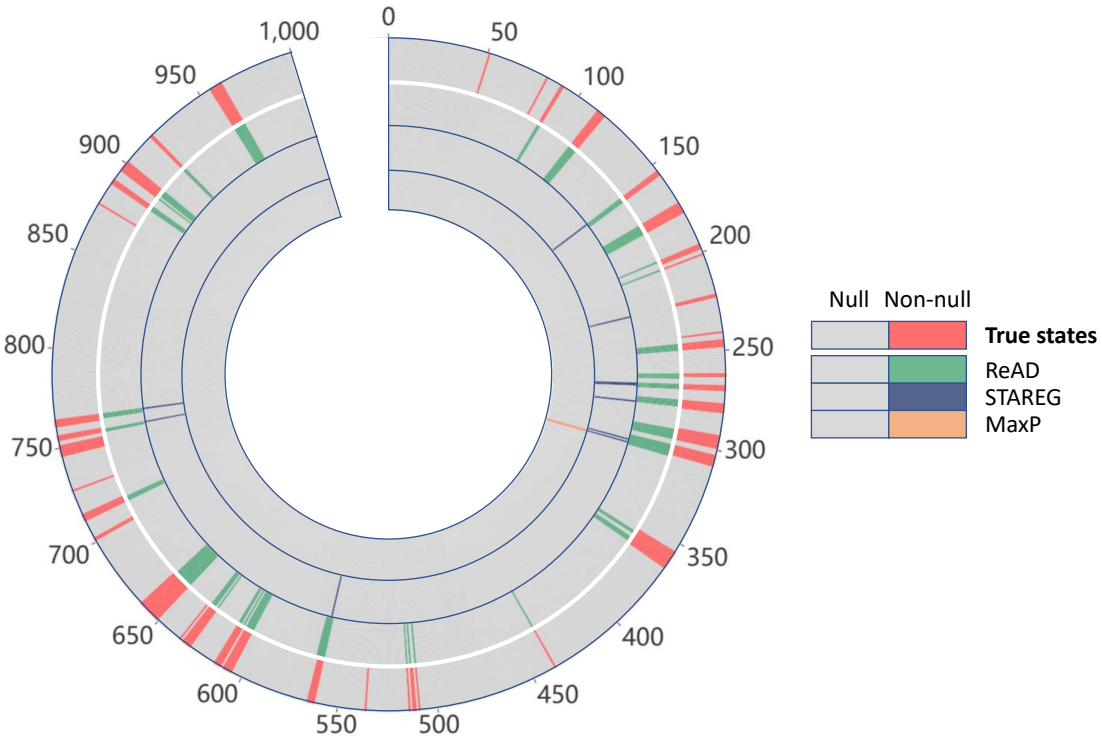

Figure 3: Methods comparison for cluster identification. Circles range from 1 (the outermost circle) to 4 (the innermost circle). The outermost circle represents true states; circle 2 represents ReAD, circle 3 represents STAREG and cirle 4 represents MaxP.

STAREG has a slight FDR inflation in some settings. By accounting for the local dependence structure via the rLIS statistic, ReAD properly controls the FDR and has substantial power gain compared to competing methods. The powers of all methods increase as μ_2 increases.

The forward-backward procedure of HMM implies that a small rLIS does not occur alone, but in clusters. Therefore, ReAD tends to identify the entire cluster of genotype-phenotype associations. Such clusters are unlikely to occur by chance and are more plausible biological signals. To illustrate this, p-values for two studies are generated following the above strategy by setting $a_{00} = 0.9, a_{33} = 0.7$, and $\mu_2 = 2$. We compare three methods for testing the composite replicability null hypotheses across two studies: the MaxP method (Benjamini et al., 2009), the STAREG method (Li et al., 2023), and the ReAD method. Figure 3 presents results of different methods in one replication. It can be seen that MaxP is extremely conservative,

medRxiv preprint doi: https://doi.org/10.1101/2023.09.04.23295018; this version posted September 5, 2023. The copyright holder for this preprint (which was not certified by peer review) is the author/funder, who has granted medRxiv a license to display the preprint in perpetuity. All rights reserved. No reuse allowed without permission.

which only identifies one single signal; STAREG rejects individual hypotheses with very small p-values in both studies; whereas ReAD can identify clusters of replicable signals.

2.2.2 Simulation II

By incorporating the LD structure in GWASs through HMM, the rLIS statistic integrates information from adjacent locations. Therefore, the rankings of SNPs based on rLIS are different from the rankings from MaxP (based on $P_{\max}$) and STAREG (based on Lfdr). We perform simulation studies to demonstrate different rankings in GWASs with realistic LD patterns among SNPs. Data for two studies are generated based on two SNP matrices from the Genetic European Variation in Disease project (Lappalainen et al., 2013). The CEU genotype data are collected from 78 Utah residents with Northern and Western European ancestry, and the FIN genotype data are measured from 89 Finnish in Finland. CEU and FIN are both sub-populations of the European Ancestry population, therefore they may have similar

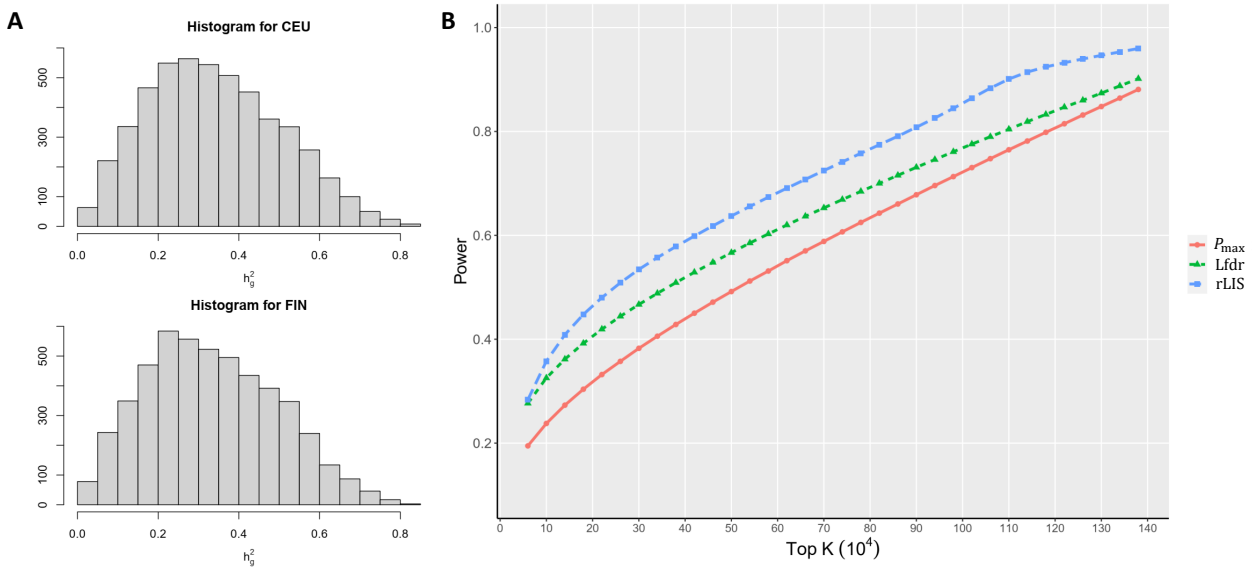

Figure 4: (A) Histogram of estimated h_g^2 for simulated CEU data and FIN data from $5,000$ runs. (B) Power of top K SNPs identified by different methods. The power is calculated as the averaged percentages of true positives selected by the top K SNPs ranked based on rLIS, Lfdr produced by STAREG, and $P_{\max}$ used in MaxP. The results are calculated from 100 runs.

medRxiv preprint doi: https://doi.org/10.1101/2023.09.04.23295018; this version posted September 5, 2023. The copyright holder for this preprint (which was not certified by peer review) is the author/funder, who has granted medRxiv a license to display the preprint in perpetuity. All rights reserved. No reuse allowed without permission.

LD structures. A detailed description of the strategy to generate continuous phenotypes corresponding to SNPs in a single gene across two studies is provided in the Methods Section. To make realistic simulations, we adjust the signal-to-noise ratio in two studies so that the SNP heritability h_g^2 is centered between 0.2 and 0.3. Figure 4(A) presents the histogram of h_g^2 for CEU and FIN studies generated from $5,000$ replications. We repeat the above data generating process to simulate GWAS data for 100 genes, resulting in $1,676,400$ pairs of p-values for corresponding SNPs. As in Wei et al. (2009), we define five adjacent SNPs on each side of the 400 causal SNPs as relevant SNPs and evaluate the performance of different replicability analysis methods by calculating the percentages of selecting relevant SNPs.

We average the percentages of true positives selected by the top K hits from 100 runs as our evaluation criterion. The power curves of different K values based on SNP rankings produced by $P_{\max}$, Lfdr and rLIS are depicted in Figure 4(B). We see that rLIS shows higher power than $P_{\max}$ and Lfdr, indicating that the rankings based on rLIS are more efficient than the rankings based on $P_{\max}$ and Lfdr in replicability analysis of GWAS data by incorporating the LD block structure through HMM.

2.3 Data analysis

2.3.1 Replicability analysis of asthma GWASs

Asthma is a complex bronchial disease characterized by chronic inflammation and narrowing of the airways, which is caused by a combination of environmental and genetic factors. The prevalence of asthma varies across different populations and ethnicities. We implement ReAD to conduct replicability analysis of asthma GWASs from the Trans-National Asthma Genetic Consortium (TAGC) and UK Biobank. The results are compared with competing methods. Demenais et al. (2018) conducted ancestry-specific meta-analyses from ethnically-diverse populations and deposited the HapMap2-imputed data in the TAGC consortium. The TAGC

medRxiv preprint doi: https://doi.org/10.1101/2023.09.04.23295018; this version posted September 5, 2023. The copyright holder for this preprint (which was not certified by peer review) is the author/funder, who has granted medRxiv a license to display the preprint in perpetuity. All rights reserved. No reuse allowed without permission.

asthma GWAS data with high-density genotyped and imputed SNP based on the European-ancestry comprises $8,843,303$ genetic variants for $19,954$ asthma cases and $107,715$ controls. UK Biobank is a large-scale prospective cohort study with over half a million participants aged 40-69 years from the United Kingdom between 2006 and 2010 (Sudlow et al., 2015). The imputed asthma GWAS from UK Biobank contains summary statistics for $8,856,162$ genetic variants measured on $39,049$ self-reported asthma cases and $298,070$ controls. We filter out SNPS with minor allele frequency (MAF) smaller than 0.05, resulting in $6,234,241$ SNPs in the TAGC study and $6,242,120$ SNPs in UK Biobank. After taking the intersection of SNPs in the two studies, we obtain paired p-values of $6,222,195$ SNPs to conduct replicability analysis.

As the *ad hoc* BH does not control FDR, we apply MaxP and STAREG on the paired p-values for comparison. The GWAS Catalog (Welter et al., 2014) reported cytogenetic regions (loci) associated with asthma. To assess the replicability of GWAS loci, we state that if at least one of the identified SNPs falls into one of the regions, the locus is identified as replicable. If a locus contains multiple significant SNPs, the SNP with the strongest association is considered as the lead SNP. For instance, if we use STAREG with Lfdr as the test statistic, the SNP with the smallest Lfdr is the lead SNP.

At FDR level 5×10^{-8}, MaxP identifies $2,853$ significant SNPs in 10 loci, which are also identified by STAREG and ReAD. Compared to MaxP, STAREG identifies 909 additional significant SNPs in 3 loci. By capturing the local LD structure through HMM, ReAD identifies $10,084$ significant SNPs in 28 genetic loci with replicable asthma associations, of which 15 loci are not detected by MaxP or STAREG. Figure 5 presents the Manhattan plots of MaxP, STAREG, and ReAD. In Figure 5, the vertical axis are $-\log_{10}$ transformations of test statistics for replicability analysis, i.e., $P_{\max}$ for MaxP, Lfdr for STAREG, and rLIS for ReAD.

medRxiv preprint doi: https://doi.org/10.1101/2023.09.04.23295018; this version posted September 5, 2023. The copyright holder for this preprint (which was not certified by peer review) is the author/funder, who has granted medRxiv a license to display the preprint in perpetuity. All rights reserved. No reuse allowed without permission.

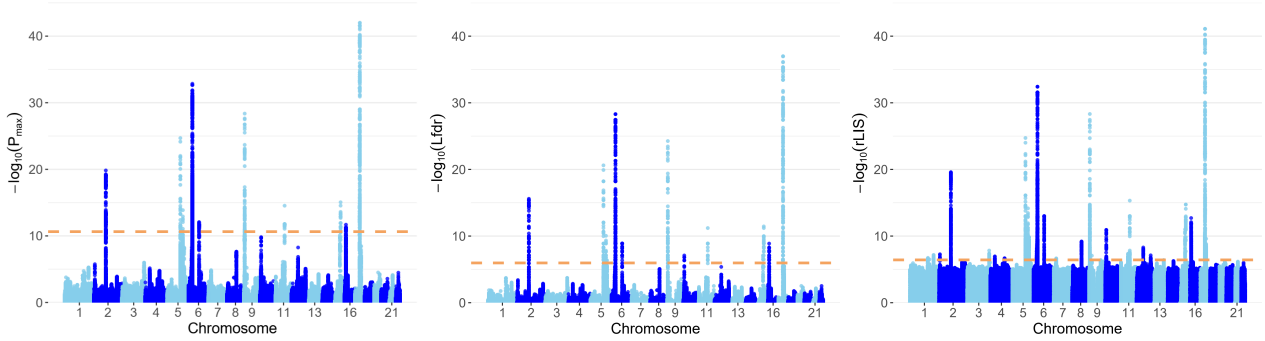

Figure 5: The Manhattan plots based on $P_{\max}$, Lfdr and rLIS. The dashed horizontal lines denote the FDR cutoffs of 5×10^{-8} produced by MaxP, STAREG, and ReAD, respectively.

Table 1: Main characteristics of the 28 loci associated with asthma in the European-ancestry TAGC and UK Biobank GWASs identified by ReAD. The SNP with the strongest association within each locus is called Lead SNP. The mapped gene denotes genes overlapping or closest to the lead SNP in the identified locus.

Locus	Lead SNP	Location of lead SNP	Mapped gene	$P_{\max}$	Lfdr	rLIS
Replicable asthma loci identified by all methods						
2q12.1	rs3771180	chr2:102,337,157	*IL18R1,IL1RL1*	1.5e-20	2.5e-16	2.5e-20
5q22.1	rs10455025	chr5:111,069,301	*BCLAF1P1,TSLP*	2.0e-25	2.4e-21	1.9e-25
5q31.1	rs20541	chr5:132,660,272	*IL13,TH2LCRR*	1.4e-14	9.1e-11	7.0e-15
6p21.32	rs17843604	chr6:32,652,506	*HLA-DQA1,HLA-DQB1*	2.2e-33	5.0e-29	3.8e-33
6p21.33	rs2596465	chr6:31,445,171	*LINC01149*	1.2e-14	4.1e-11	3.1e-15
6q15	rs2325291	chr6:90,276,967	*BACH2*	8.6e-13	1.3e-09	1.0e-13
9p24.1	rs992969	chr9:6,209,697	*GTF3AP1,IL33*	4.3e-29	5.5e-25	4.8e-29
11q13.5	rs2155219	chr11:76,588,150	*LINC02757,EMSY*	2.9e-15	6.3e-12	4.8e-16
15q22.33	rs17228058	chr15:67,157,967	*SMAD3*	2.9e-15	6.3e-12	1.8e-15
16p13.13	rs12935657	chr16:11,125,184	*CLEC16A*	2.1e-12	1.3e-09	2.0e-13
Replicable asthma loci identified by ReAD and STAREG but not by MaxP						
5q31.3	rs2338822	chr5:142,123,494	*NDFIP1*	6.0e-09	1.2e-06	1.5e-10
10p14	rs962993	chr10:9,011,169	*LINC02676*	1.9e-10	1.5e-07	1.2e-11
15q22.2	rs11071558	chr15:60,777,222	*RORA*	8.3e-11	8.1e-08	9.9e-12
Replicable asthma loci only identified by ReAD						

medRxiv preprint doi: https://doi.org/10.1101/2023.09.04.23295018; this version posted September 5, 2023. The copyright holder for this preprint (which was not certified by peer review) is the author/funder, who has granted medRxiv a license to display the preprint in perpetuity. All rights reserved. No reuse allowed without permission.

1q32.1	rs7555556	chr1:203,121,848	*ADORA1*	5.5e-06	9.3e-04	6.9e-08
1q21.3	rs4845623	chr1:154,443,301	*IL6R*	1.5e-04	5.1e-04	2.7e-07
1q24.2	rs864537	chr1:167,442,147	*CD247*	3.2e-05	3.0e-03	3.2e-07
2p25.1	rs10174949	chr2:8,302,118	*LINC00299*	3.0e-06	5.7e-04	5.3e-08
3q28	rs2889896	chr3:188,384,928	*LPP*	1.0e-06	1.9e-04	1.5e-08
4p14	rs6815814	chr4:38,814,717	*TLR1*	1.2e-05	1.7e-03	1.3e-07
4q27	rs1904522	chr4:122,415,763	*ADAD1*	1.7e-05	2.5e-03	2.3e-07
6p22.1	rs2523716	chr6:30,202,748	*TRIM26*	1.4e-08	4.6e-06	3.5e-10
8q21.13	rs10957979	chr8:80,377,552	*RNU6-1213P*	2.3e-08	8.6e-06	6.5e-10
11q12.2	rs174541	chr11:61,798,436	*FADS2*	2.3e-06	5.6e-04	4.4e-08
12q13.3	rs324014	chr12:57,116,526	*STAT6*	2.7e-07	6.0e-05	5.1e-09
12q24.31	rs625228	chr12:120,840,463	*SPPL3*	9.0e-06	5.8e-04	7.7e-08
17q21.33	rs17637472	chr17:49,384,071	*ZNF652,PHB*	3.3e-09	3.3e-06	2.5e-10
17q21.32	rs12949836	chr17:49,271,490	*FLJ40194*	1.6e-07	6.0e-05	4.6e-09
17q21.2	rs34349578	chr17:42,446,111	*ATP6V0A1,RNU7-97P*	5.6e-05	1.0e-03	1.9e-07

Table 1 displays main characteristics of the 28 cytogenetic regions identified by ReAD. The mapped gene denotes genes overlapping or closest to the lead SNP in the identified locus. The 15 loci only identified by ReAD harbor signals closely related to asthma. For example, the lead SNP in locus 2p25.1, rs10174949, is in the intron of gene *LINC00299* and plays an important role in atopic dermatitis, including asthma, hay fever and eczema in European and UK populations (Zhu et al., 2020, 2018; Ferreira et al., 2017). The 8q21.13 region is reported to be associated with asthma and hay fever in a European-ancestry study (Ferreira et al., 2014). The lead SNP rs6473226 lies between gene *MIR5708* (chr8:80,241,389–80,241,473) and gene *RNU6-1213P* (chr8:80,405,516–80,405,609), and its association with asthma has been observed in several European-ancestry studies (Demenais et al., 2018; Olafsdottir et al., 2020).

medRxiv preprint doi: https://doi.org/10.1101/2023.09.04.23295018; this version posted September 5, 2023. The copyright holder for this preprint (which was not certified by peer review) is the author/funder, who has granted medRxiv a license to display the preprint in perpetuity. All rights reserved. No reuse allowed without permission.

2.3.2 Replicability analysis of ulcerative colitis GWASs

Inflammatory bowel disease is a chronic, relapsing intestinal inflammatory disease. It has the highest age-standardized prevalence rate in the US followed by the UK (Alatab et al., 2020) with increasing prevalence in Asia and developing countries (Molodecky et al., 2012). Ulcerative colitis (UC) is one of the two main forms of inflammatory bowel disease. We conduct replicability analysis of GWASs from the International Inflammatory Bowel Disease Genetics Consortium (IIBDGC) and the UK Biobank. The IIBDGC GWAS analyses $8,857,076$ SNPs from $6,968$ UC cases and $20,464$ population controls of European descent (Liu et al., 2015). The imputed UK Biobank GWAS data contain summary statistics of $8,856,162$ SNPs genotyped on $1,795$ self-reported UC cases and $335,324$ controls from the United Kingdom. We filter out SNPs with MAF smaller than 0.05, resulting in $6,243,744$ SNPs in the IIBDGC study and $6,242,120$ SNPs in the UK Biobank. We use the paired p-values of $6,232,147$ SNPs common to both studies as input for replicability analysis.

We apply MaxP, STAREG, and ReAD on the paired p-values. At FDR level 5×10^{-8}, MaxP identifies $1,239$ significant SNPs in 1 locus. STAREG identifies $1,542$ significant SNPs in 2 loci, one of which is also detected by MaxP. ReAD identifies $3,307$ significant SNPs in 7 genetic loci, including 5 loci that are not detected by MaxP or STAREG. Figure 6 presents the Manhattan plots of MaxP, STAREG and ReAD.

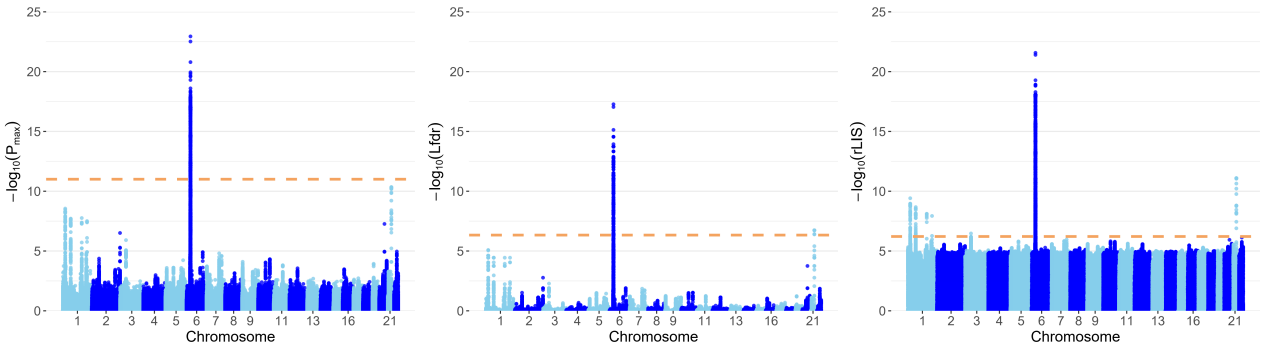

Figure 6: The Manhattan plots based on $P_{\max}$, Lfdr and rLIS. The dashed horizontal lines denote the FDR cutoffs of 5×10^{-8} produced by MaxP, STAREG, and ReAD, respectively.

medRxiv preprint doi: https://doi.org/10.1101/2023.09.04.23295018; this version posted September 5, 2023. The copyright holder for this preprint (which was not certified by peer review) is the author/funder, who has granted medRxiv a license to display the preprint in perpetuity. All rights reserved. No reuse allowed without permission.

We assess the replicability of genetic loci identified by different methods in GWAS Catalog (Welter et al., 2014). Table 2 presents the main characteristics of the 7 replicable genetic loci identified by ReAD. UC associations of these loci in cohorts of European descent have been repored in the literature. For instance, the lead SNP of loci 6p21.32, rs6927022, is in the intron of gene *HLA-DQA1*, and the HLA complex is associated with multiple risk alleles for inflammatory bowel disease, including UC (Nowak et al., 2021; Reinshagen et al., 1996; Ashton et al., 2019). The lead SNP harbored in loci 1q23.3, rs1801274, is only identified by ReAD, and has confirmed associations with UC in several European-ancestry studies (Liu et al., 2015; De Lange et al., 2017; Anderson et al., 2011). We have additional validations in DisGeNET, a versatile platform that contains a comprehensive catalog of genes and variants associated with human diseases (Piñero et al., 2015). Many mapped genes of the lead SNP only identified by ReAD have been reported to be associated with UC, such as gene *FCGR2A* in locus 1q23.3, gene *IL23R* in locus 1p31.3, gene *IL10* in locus 1q32.1, and gene *MST1* in locus 3p21.31.

3 Discussion

In this paper, we present ReAD, an efficient method accounting for the LD structure to identify replicable associations from two GWASs datasets. We conduct extensive simulation studies and analyze two GWAS datasets. Compared to conventional approaches that impose independence assumption among SNPs, ReAD provides effective FDR control. It has a substantial power gain in identifying genuine and replicable genetic loci. It is computationally scalable to hundreds of millions of SNPs and has no tuning parameters.

In this paper, our discussion mainly focuses on assessing the replicability of each SNP within a genomic locus. We acknowledge that, in the applications of genetic association analysis, varying LD patterns between studies can lead to inconsistent significant findings at the

medRxiv preprint doi: https://doi.org/10.1101/2023.09.04.23295018; this version posted September 5, 2023. The copyright holder for this preprint (which was not certified by peer review) is the author/funder, who has granted medRxiv a license to display the preprint in perpetuity. All rights reserved. No reuse allowed without permission.

Table 2: Main characteristics of the 7 loci associated with UC in the European-ancestry IIBDGC and UK Biobank GWASs identified by ReAD. The SNP with the strongest association within each locus is called the lead SNP. The mapped gene denotes genes overlapping or closest to the lead SNP in the identified locus.

Locus	Lead SNP	Location of lead SNP	Mapped gene	$P_{\max}$	Lfdr	rLIS
Replicable asthma loci identified by all methods						
6p21.32	rs6927022	chr6:32,644,620	*HLA-DQA1*	1.1e-20	2.8e-15	1.2e-19
Replicable asthma loci identified by ReAD and STAREG but not by MaxP						
21q22.2	rs2836882	chr21:39,094,644	*RPL23AP12*	4.5e-11	1.9e-07	8.1e-12
Replicable asthma loci only identified by ReAD						
1p36.13	rs4654903	chr1:19,874,497	*RNF186, OTUD3*	1.3e-08	3.6e-05	6.7e-09
1q23.3	rs1801274	chr1:161,509,955	*FCGR2A*	1.7e-08	3.6e-05	7.7e-09
1p31.3	rs2201841	chr1:67,228,519	*C1orf141, IL23R*	6.1e-08	1.8e-04	1.8e-08
1q32.1	rs3024505	chr1:206,766,559	*Y_RNA, IL10*	4.1e-08	8.9e-05	5.4e-07
3p21.31	rs3197999	chr3:49,684,099	*MST1*	1.2e-06	5.2e-03	3.4e-07

SNP level. Hence scientifically, a more relevant question should be the consistency of underlying association signals within each interrogated locus across original and replication studies. To this end, we apply a simple and practical strategy requiring at least one SNP-level findings replicable. With the potential varying LD structures fully accounted for by the proposed HMM, we find this strategy intuitive and effective when applied to genomic loci with proper resolutions (as illustrated by our simulations and real data examples). Nevertheless, this locus-level criterion may be considered overly lenient. We will continue to explore alternative locus-level replicability assessment criteria in our future work.

In this work, we use repeated significance to assess replicability. We note that applying such a replicability criterion is debatable in the scientific community. While acknowledging its drawbacks, especially its conservativeness, we note the following context-specific factors. First, despite continued efforts to include more informative statistics summarizing GWAS findings, a large body of historical GWAS findings are *only* reported in p-values (See GWAS

medRxiv preprint doi: https://doi.org/10.1101/2023.09.04.23295018; this version posted September 5, 2023. The copyright holder for this preprint (which was not certified by peer review) is the author/funder, who has granted medRxiv a license to display the preprint in perpetuity. All rights reserved. No reuse allowed without permission.

catalog (Welter et al., 2014)), which fundamentally limits applying alternative replicability criteria. Second, because complicated unknown confoundings, e.g., population stratification and unobserved batch effects in genotyping experiments, often cause false positives in genetic association analysis, the genetics community has consistently advocated conservative replicability criteria to ensure the reliability of GWAS findings (Skol et al., 2006; McGuire et al., 2021). Third, we emphasize that our main statistical contribution is to account for the correlation structure between genetic variants, and our work can be naturally extended to applying other alternative replicability criteria.

On a related point, although we exclusively assume that GWAS results are reported in the form of single-SNP testing p-values throughout this paper, the proposed statistical methodology can be extended to other forms of summary statistics. For example, probabilistic fine-mapping analysis of genetic association signals has become increasingly popular, thanks to the availability of efficient variable selection algorithms (Benner et al., 2016; Wang et al., 2020; Wen et al., 2016). The fine-mapping result is typically given as a posterior inclusion probability (PIP) at the individual SNP level. With the ability to construct a Bayesian credible set for each underlying signal within a genomic locus, the PIPs have many advantages over single-SNP p-values. Theoretically, our work can be straightforwardly extended to this setting by noting the connection that $1 - \text{PIP}$ is equivalent to the local fdr in the Bayesian perspective. We will leave this extension to our future work.

4 Methods

4.1 The hidden Markov model for replicability analysis

Suppose there are J SNPs in two independent GWASs. We are interested in testing whether the jth SNP is associated with the phenotype in both studies. Let θ_{ij} denote the inferred

medRxiv preprint doi: https://doi.org/10.1101/2023.09.04.23295018; this version posted September 5, 2023. The copyright holder for this preprint (which was not certified by peer review) is the author/funder, who has granted medRxiv a license to display the preprint in perpetuity. All rights reserved. No reuse allowed without permission.

association status of SNP j in study i, where $\theta_{ij} = 1$ indicates the jth SNP ($j = 1, \ldots, J$) is inferred associated with the phenotype in study i ($i = 1, 2$) and $\theta_{ij} = 0$ otherwise. We use s_j ($j = 1, \ldots, J$) to denote the joint status.

$$s_j = \begin{cases} 0, & (\theta_{1j}, \theta_{2j}) = (0, 0), \\ 1, & (\theta_{1j}, \theta_{2j}) = (0, 1), \\ 2, & (\theta_{1j}, \theta_{2j}) = (1, 0), \\ 3, & (\theta_{1j}, \theta_{2j}) = (1, 1). \end{cases}$$

The replicability null hypotheses is

$$H_{0j} : s_j \in \{0, 1, 2\}, j = 1, \ldots, J. \tag{1}$$

Let $\boldsymbol{p}_i = (p_{ij})_{j=1}^J$ denote p-values of J SNPs in study i. We use mixture models for the conditional distributions of p-values given θ values. Specifically,

$$\begin{aligned} p_{1j}|\theta_{1j} &\sim (1 - \theta_{1j}) f_0 + \theta_{1j} f_1, \\ p_{2j}|\theta_{2j} &\sim (1 - \theta_{2j}) f_0 + \theta_{2j} f_2, \end{aligned} \tag{2}$$

where f_0 is the probability density function of p-values when $\theta_{1j} = \theta_{2j} = 0$, and f_1 and f_2 are the p-value density functions under non-null in study 1 and study 2, respectively. We assume f_0 follows the standard uniform distribution and impose the following monotone likelihood ratio condition (Sun and Cai, 2007; Cao et al., 2013, 2022).

$$f_1(x)/f_0(x) \text{ and } f_2(x)/f_0(x) \text{ are monotonically non-increasing in } x. \tag{3}$$

This condition naturally arises as small p-values indicate evidence against the null. To capture

medRxiv preprint doi: https://doi.org/10.1101/2023.09.04.23295018; this version posted September 5, 2023. The copyright holder for this preprint (which was not certified by peer review) is the author/funder, who has granted medRxiv a license to display the preprint in perpetuity. All rights reserved. No reuse allowed without permission.

the LD structure among SNPs, we assume that $\boldsymbol{s} = (s_1, \ldots, s_J)$ follows a four-state stationary, irreducible, and aperiodic hidden Markov model (HMM). The transition probabilities

$$a_{kl} = \mathbb{P}(s_{j+1} = l | s_j = k) \tag{4}$$

for $k, l = 0, 1, 2, 3$ with constraint $\sum_{l=0}^{3} a_{kl} = 1$. The stationary distribution of each state s_j is $\mathbb{P}(s_j = k) = \pi_k$ for $k = 0, 1, 2, 3$ and $\sum_{k=0}^{3} \pi_k = 1$. The paired p-values for the jth SNP are assumed to be conditionally independent satisfying

$$f(p_{1j}, p_{2j} | \theta_{1j}, \theta_{2j}) = f(p_{1j} | \theta_{1j}) f(p_{2j} | \theta_{2j}).$$

Based on the mixture model (2), we have

$$f^{(s_j)}(p_{1j}, p_{2j}) = \begin{cases} f_0(p_{1j}) f_0(p_{2j}), & s_j = 0, \\ f_0(p_{1j}) f_2(p_{2j}), & s_j = 1, \\ f_1(p_{1j}) f_0(p_{2j}), & s_j = 2, \\ f_1(p_{1j}) f_2(p_{2j}), & s_j = 3. \end{cases}$$

Denote by $\mathcal{A} = \{a_{kl} : k, l = 0, 1, 2, 3\}$ the transition matrix, $\boldsymbol{\pi} = (\pi_0, \pi_1, \pi_2, \pi_3)$ the vector of stationary distribution, and $\mathcal{F} = \left(f^{(0)}, f^{(1)}, f^{(2)}, f^{(3)}\right)$ the probability density functions of the bivariate observations (p_{1j}, p_{2j}). The convergence theorem of a Markov chain (Theorem 5.5.1 in Durrett (2019)) implies that

$$\frac{1}{J} \sum_{j=1}^{J} I(s_j = k) \to \pi_k$$

almost surely for $k = 0, 1, 2, 3$ as $J \to \infty$. As f_0 is assumed to follow a standard uniform distribution, we use $\boldsymbol{\lambda} = (\boldsymbol{\pi}, \mathcal{A}, f_1, f_2)$ to denote the collection of unknown parameters and functions in the HMM. Our goal is to separate the replicable SNPs ($s_j = 3$) from the non-

medRxiv preprint doi: https://doi.org/10.1101/2023.09.04.23295018; this version posted September 5, 2023. The copyright holder for this preprint (which was not certified by peer review) is the author/funder, who has granted medRxiv a license to display the preprint in perpetuity. All rights reserved. No reuse allowed without permission.

312 replicable SNPs ($s_j \in \{0, 1, 2\}$) based on the observed bivariate p-values.

313 4.2 FDR control for replicability analysis accounting for LD

314 4.2.1 The rLIS statistic for replicability analysis across two studies

Consider the ideal setup that an oracle knows $\boldsymbol{\lambda} = (\boldsymbol{\pi}, \mathcal{A}, f_1, f_2)$. We define the replicability local index of significance (rLIS) as the posterior probability of being null. Specifically,

$$\text{rLIS}_j := \mathbb{P}_{\boldsymbol{\lambda}} \left(s_j \in \{0, 1, 2\} | \boldsymbol{p}_1, \boldsymbol{p}_2 \right).$$

Given $\boldsymbol{\lambda}$, the forward and backward probabilities are defined as $\alpha_j(s_j) = \mathbb{P}_{\boldsymbol{\lambda}} \left((p_{1t}, p_{2t})_{t=1}^{j}, s_j \right)$ and $\beta_j(s_j) = \mathbb{P}_{\boldsymbol{\lambda}} \left((p_{1t}, p_{2t})_{t=j+1}^{J} \mid s_j \right)$, respectively. The forward-backward procedure (Baum et al., 1970) can be used in the calculation. Specifically, we initialize $\alpha_1(s_1) = \pi_{s_1} f^{(s_1)}(p_{11}, p_{21})$ and $\beta_J(s_J) = 1$. We can obtain $\alpha_j(\cdot)$ and $\beta_j(\cdot)$ for $j = 1, \ldots, J$ recursively by

$$\alpha_{j+1}(s_{j+1}) = \sum_{s_j=0}^{3} \alpha_j(s_j) a_{s_j s_{j+1}} f^{(s_{j+1})}(p_{1,j+1}, p_{2,j+1})$$

and

$$\beta_j(s_j) = \sum_{s_{j+1}=0}^{3} \beta_{j+1}(s_{j+1}) f^{(s_{j+1})}(p_{1,j+1}, p_{2,j+1}) a_{s_j s_{j+1}}.$$

Hence we have

$$\text{rLIS}_j = \frac{\sum_{s_j=0}^{2} \alpha_j(s_j)\beta_j(s_j)}{\sum_{s_j=0}^{3} \alpha_j(s_j)\beta_j(s_j)}.$$

The rejection rule can be written as

$$\delta_j = I(\text{rLIS}_j \leq t), \;\; j = 1, \ldots, J,$$

medRxiv preprint doi: https://doi.org/10.1101/2023.09.04.23295018; this version posted September 5, 2023. The copyright holder for this preprint (which was not certified by peer review) is the author/funder, who has granted medRxiv a license to display the preprint in perpetuity. All rights reserved. No reuse allowed without permission.

where $I(\cdot)$ is the indicator function.

We next derive the threshold $\hat{t}$ for a pre-specified FDR level q. Total number of discoveries and the number of false discoveries are $R(t) = \sum_{j=1}^{J} I(\text{rLIS}_j \leq t)$ and $V(t) = \sum_{j=1}^{J} I(\text{rLIS}_j \leq t, s_j \in \{0,1,2\})$, respectively. We have

$$\begin{aligned}\mathbb{E}[V(t)] &= \mathbb{E}\left[\sum_{j=1}^{J}\{\pi_0 I(\text{rLIS}_j \leq t|s_j = 0) + \pi_1 I(\text{rLIS}_j \leq t|s_j = 1) + \pi_2 I(\text{rLIS}_j \leq t|s_j = 2)\}\right] \\ &= \mathbb{E}\left[\sum_{j=1}^{J} I(\text{rLIS}_j \leq t)\text{rLIS}_j\right].\end{aligned}$$

Let $\text{rLIS}_{(1)} \leq \text{rLIS}_{(2)} \leq \cdots \leq \text{rLIS}_{(J)}$ be the order statistics and $H_{(1)}, \ldots, H_{(J)}$ be the corresponding hypotheses. If k hypotheses are rejected, the number of false discoveries can be estimated by

$$\widehat{V}(k) = \sum_{j=1}^{k} \text{rLIS}_{(k)},$$

and the FDR can be estimated by $\frac{1}{k}\sum_{j=1}^{k} \text{rLIS}_{(j)}$. We shall use the following step-up procedure to control the FDR at level q (Sun and Cai, 2009).

$$\text{let } \hat{k} = \max\left\{k : \frac{1}{k}\sum_{j=1}^{k} \text{rLIS}_{(j)} \leq q\right\};$$

$$\text{then reject all } H_{(j)} \text{ for } j = 1, \ldots, \hat{k}.$$

We provide an estimation of $\boldsymbol{\lambda}$ in the next section.

4.2.2 Data-driven testing procedure

To estimate the unknown parameters and functions in $\boldsymbol{\lambda}$, we first define two posterior probabilities $\gamma_j(s_j) = \mathbb{P}_{\boldsymbol{\lambda}}(s_j \mid \boldsymbol{p}_1, \boldsymbol{p}_2)$ and $\xi_j(s_j, s_{j+1}) = \mathbb{P}_{\boldsymbol{\lambda}}(s_j, s_{j+1} \mid \boldsymbol{p}_1, \boldsymbol{p}_2)$. By the definition, $\gamma_j(s_j) = \sum_{s_{j+1}=0}^{3} \xi_j(s_j, s_{j+1})$. They can be obtained from the forward and backward probabil-

medRxiv preprint doi: https://doi.org/10.1101/2023.09.04.23295018; this version posted September 5, 2023. The copyright holder for this preprint (which was not certified by peer review) is the author/funder, who has granted medRxiv a license to display the preprint in perpetuity. All rights reserved. No reuse allowed without permission.

ities

$$\gamma_j(s_j) = \frac{\alpha_j(s_j)\beta_j(s_j)}{\sum_{s_j=0}^{3} \alpha_j(s_j)\beta_j(s_j)}$$

and

$$\xi_j(s_j, s_{j+1}) = \frac{\alpha_j(s_j)\beta_{j+1}(s_{j+1})a_{s_j s_{j+1}} f^{(s_{j+1})}(p_{1,j+1}, p_{2,j+1})}{\sum_{s_j=0}^{3}\sum_{s_{j+1}=0}^{3} \alpha_j(s_j)\beta_{j+1}(s_{j+1})a_{s_j s_{j+1}} f^{(s_{j+1})}(p_{1,j+1}, p_{2,j+1})}.$$

The likelihood function of the complete data $(\boldsymbol{p}_1, \boldsymbol{p}_2, \boldsymbol{s})$ is given by

$$L\left(\boldsymbol{\lambda}; \boldsymbol{p}_1, \boldsymbol{p}_2, \boldsymbol{s}\right) = \pi_{s_1} \prod_{j=2}^{J} a_{s_{j-1}s_j} \cdot \prod_{j=1}^{J} f^{(s_j)}(p_{1j}, p_{2j}).$$

We develop a non-parametric EM algorithm (Dempster et al., 1977) to estimate the unknowns $\boldsymbol{\lambda} = (\boldsymbol{\pi}, \mathcal{A}, f_1, f_2)$ under the monotone likelihood ratio constraint (3). With an appropriate initialization of the unknowns, $\boldsymbol{\lambda}^{(0)} = \left(\boldsymbol{\pi}^{(0)}, \mathcal{A}^{(0)}, f_1^{(0)}, f_2^{(0)}\right)$, the EM algorithm proceeds by iteratively implementing the following two steps.

E-step: Given current $\boldsymbol{\lambda}^{(t)} = \left(\boldsymbol{\pi}^{(t)}, \mathcal{A}^{(t)}, f_1^{(t)}, f_2^{(t)}\right)$, the forward and backward probabilities $\alpha_j^{(t)}(s_j), \beta_j^{(t)}(s_j)$ and the posterior probabilities $\gamma_j^{(t)}(s_j), \xi_j^{(t)}(s_j, s_{j+1})$ are calculated. The conditional expectation of the log-likelihood function can be written as

$$\begin{aligned} D\left(\boldsymbol{\lambda}|\boldsymbol{\lambda}^{(t)}\right) &= \sum_{\boldsymbol{s}} \mathbb{P}_{\boldsymbol{\lambda}^{(t)}}(\boldsymbol{s}|\boldsymbol{p}_1, \boldsymbol{p}_2) \log L\left(\boldsymbol{\lambda}; \boldsymbol{p}_1, \boldsymbol{p}_2, \boldsymbol{s}\right) \\ &= \sum_{\boldsymbol{s}} \left\{ \mathbb{P}_{\boldsymbol{\lambda}^{(t)}}(\boldsymbol{s}|\boldsymbol{p}_1, \boldsymbol{p}_2) \left[\log \pi_{s_1} + \sum_{j=2}^{J} \log a_{s_{j-1}s_j} + \sum_{j=1}^{J} \log f^{(s_j)}(p_{1j}, p_{2j}) \right] \right\}. \end{aligned}$$

M-step: Update $\boldsymbol{\lambda}^{(t+1)}$ by

$$\boldsymbol{\lambda}^{(t+1)} = \arg \max_{\boldsymbol{\pi}, \mathcal{A}, f_1, f_2} D\left(\boldsymbol{\pi}, \mathcal{A}, f_1, f_2 | \boldsymbol{\lambda}^{(t)}\right).$$

medRxiv preprint doi: https://doi.org/10.1101/2023.09.04.23295018; this version posted September 5, 2023. The copyright holder for this preprint (which was not certified by peer review) is the author/funder, who has granted medRxiv a license to display the preprint in perpetuity. All rights reserved. No reuse allowed without permission.

We can update each component alternatingly. By using the Lagrange multiplier, we can calculate $\boldsymbol{\pi}^{(t+1)}$ and $\mathcal{A}^{(t+1)}$ as

$$\pi_s^{(t+1)} = \gamma_1^{(t)}(s), s \in \{0, 1, 2, 3\}$$

and

$$a_{kl}^{(t+1)} = \frac{\sum_{j=2}^{J} \xi_{j-1}^{(t)}(k, l)}{\sum_{j=2}^{J} \sum_{l=0}^{3} \xi_{j-1}^{(t)}(k, l)}, k, l \in \{0, 1\}.$$

The two functions can be updated by

$$f_1^{(t+1)} = \arg\max_{f_1 \in \mathbb{H}} \left\{ \sum_{j=1}^{J} \left[\gamma_j^{(t)}(2) + \gamma_j^{(t)}(3) \right] \log f_1(p_{1j}) \right\} \tag{5}$$

and

$$f_2^{(t+1)} = \arg\max_{f_2 \in \mathbb{H}} \left\{ \sum_{j=1}^{J} \left[\gamma_j^{(t)}(1) + \gamma_j^{(t)}(3) \right] \log f_2(p_{2j}) \right\}, \tag{6}$$

where $\mathbb{H}$ is a set of monotonic non-increasing density functions (Sun and Cai, 2007; Cao et al., 2013, 2022). We solve (5) and (6) independently using the non-parametric maximum likelihood estimation implemented with PAVA (Robertson et al., 1988).

The **E-step** and **M-step** are conducted iteratively until convergence. Detailed derivations of the algorithm are presented in the Supplemental Note A. With the estimate $\hat{\boldsymbol{\lambda}} = \{\hat{\boldsymbol{\pi}}, \hat{\mathcal{A}}, \hat{f}_1, \hat{f}_2\}$, we can calculate the test statistics $\widehat{\text{rLIS}}_j = \mathbb{P}_{\hat{\boldsymbol{\lambda}}}(s_j \in \{0, 1, 2\} | \boldsymbol{p}_1, \boldsymbol{p}_2)$. Let $\widehat{\text{rLIS}}_{(1)} \leq \cdots \leq \widehat{\text{rLIS}}_{(J)}$ be the order statistics of $\widehat{\text{rLIS}}_j$, and denote $H_{(1)}, \ldots, H_{(J)}$ as the

medRxiv preprint doi: https://doi.org/10.1101/2023.09.04.23295018; this version posted September 5, 2023. The copyright holder for this preprint (which was not certified by peer review) is the author/funder, who has granted medRxiv a license to display the preprint in perpetuity. All rights reserved. No reuse allowed without permission.

corresponding H_{0j}. The data-driven testing procedure works as follows.

$$\text{Let } \hat{k} = \max\left\{ i : \frac{1}{i}\sum_{j=1}^{i} \widehat{\text{rLIS}}_{(j)} \leq q \right\},$$

$$\text{and reject } H_{(i)} \text{ for } i = 1, \ldots, \hat{k}.$$

4.3 Realistic simulation design

In simulation II, we perform realistic simulations to show the rankings of SNPs using rLIS in two GWASs, where LD structures are derived from real data. Based on the CEU genotype data and FIN genotype data from the Genetic European Variation in Disease project (Lappalainen et al., 2013), we filter out SNPs with the same genotypes in all samples and obtain genotypes of $16,764$ SNPs in both studies. We specify 5 causal SNPs in each study, 4 of which are the same in the two studies. Two of the 4 causal SNPs are close (separated by five SNPs), and the other SNPs are selected randomly. Then in each study, for the ith subject ($i = 1, \ldots, 78$ in the CEU study and $i = 1, \ldots, 89$ in the FIN study), we generate continuous phenotypes using the linear regression model

$$y_i = \beta_0 + \sum_{k=1}^{5} G_{ik}^c \beta_k + \epsilon_i,$$

where β_0 is the intercept term, $G_{i1}^c, \ldots, G_{i5}^c$ are the genotypes of the ith subject for the 5 causal SNPs, $\beta_1, \ldots, \beta_5$ are regression coefficients, and ϵ_i is an error term generated from $N(0, 1)$, a standard normal distribution. The intercept term and the regression coefficients of causal SNPs $\beta_k, k = 0, 1, \ldots, 5$, follow $N(0, \sigma^2)$, a normal distribution with mean 0 and standard deviation σ. We set $\sigma = 0.6$ such that the SNP heritability h_g^2, similar in spirit to the R^2 in linear regression models, is centered between 0.2 and 0.3. p-values are obtained by a marginal regression of each SNP on the phenotype. We repeat the above process 100 times

medRxiv preprint doi: https://doi.org/10.1101/2023.09.04.23295018; this version posted September 5, 2023. The copyright holder for this preprint (which was not certified by peer review) is the author/funder, who has granted medRxiv a license to display the preprint in perpetuity. All rights reserved. No reuse allowed without permission.

to get p-values of $1,676,400$ SNPs.

4.4 Computation time

We compare the computation time of different methods. All methods are implemented in R, in which STAREG and ReAD use Rcpp to speed up the computation. All computations are carried out in an Intel(R) Core(TM) i7-9750H 2.6GHz CPU with 64 GB RAM laptop. Table 3 summarizes the results. We observe that all methods are quick to compute. The additional time that ReAD takes in simulation studies is negligible in practice.

Table 3: Computation time (in seconds) of different methods.

Dataset	# of SNPs	MaxP	STAREG	ReAD
Simulation I	$10,000$	0.0033	0.0165	0.1871
Simulation II	$1,676,400$	0.1897	3.7237	35.159
Asthma	$6,222,195$	0.7317	169.82	105.47
UC	$6,232,147$	0.7428	9.5248	83.974

References

S. Alatab, S. G. Sepanlou, and et al. The global, regional, and national burden of inflammatory bowel disease in 195 countries and territories, 1990–2017: a systematic analysis for the global burden of disease study 2017. *The Lancet Gastroenterology and Hepatology*, 5(1): 17–30, 2020.

C. A. Anderson, G. Boucher, C. W. Lees, A. Franke, M. D'Amato, K. D. Taylor, J. C. Lee, P. Goyette, M. Imielinski, A. Latiano, et al. Meta-analysis identifies 29 additional ulcerative colitis risk loci, increasing the number of confirmed associations to 47. *Nature Genetics*, 43 (3):246–252, 2011.

medRxiv preprint doi: https://doi.org/10.1101/2023.09.04.23295018; this version posted September 5, 2023. The copyright holder for this preprint (which was not certified by peer review) is the author/funder, who has granted medRxiv a license to display the preprint in perpetuity. All rights reserved. No reuse allowed without permission.

J. J. Ashton, K. Latham, R. M. Beattie, and S. Ennis. the genetics of the human leucocyte antigen region in inflammatory bowel disease. *Alimentary Pharmacology & Therapeutics*, 50(8):885–900, 2019.

L. E. Baum, T. Petrie, G. Soules, and N. Weiss. A maximization technique occurring in the statistical analysis of probabilistic functions of markov chains. *Annals of Mathematical Statistics*, 41(1):164–171, 1970.

C. G. Begley and L. M. Ellis. Raise standards for preclinical cancer research. *Nature*, 483 (7391):531–533, 2012.

Y. Benjamini and Y. Hochberg. Controlling the false discovery rate: a practical and powerful approach to multiple testing. *Journal of the Royal Statistical Society: Series B (Methodological)*, 57(1):289–300, 1995.

Y. Benjamini, R. Heller, and D. Yekutieli. Selective inference in complex research. *Philosophical Transactions of the Royal Society A: Mathematical, Physical and Engineering Sciences*, 367(1906):4255–4271, 2009.

C. Benner, C. C. Spencer, A. S. Havulinna, V. Salomaa, S. Ripatti, and M. Pirinen. Finemap: efficient variable selection using summary data from genome-wide association studies. *Bioinformatics*, 32(10):1493–1501, 2016.

M. Bogomolov and R. Heller. Replicability across multiple studies. *arXiv preprint arXiv:2210.00522*, 2022.

F. M. Busing. Monotone regression: A simple and fast o(n) pava implementation. *Journal of Statistical Software*, 102:1–25, 2022.

H. Cao, W. Sun, and M. R. Kosorok. The optimal power puzzle: scrutiny of the monotone likelihood ratio assumption in multiple testing. *Biometrika*, 100(2):495–502, 2013.

medRxiv preprint doi: https://doi.org/10.1101/2023.09.04.23295018; this version posted September 5, 2023. The copyright holder for this preprint (which was not certified by peer review) is the author/funder, who has granted medRxiv a license to display the preprint in perpetuity. All rights reserved. No reuse allowed without permission.

H. Cao, J. Chen, and X. Zhang. Optimal false discovery rate control for large scale multiple testing with auxiliary information. *Annals of Statistics*, 50(2):807–857, 2022.

S. J. Chanock, T. Manolio, L. D. Brooks, L. R. Cardon, M. Daly, and P. Donnelly. Replicating genotype-phenotype associations. *Nature (London)*, 447(7145):655–660, 2007.

D. Chung, C. Yang, C. Li, J. Gelernter, and H. Zhao. Gpa: a statistical approach to prioritizing gwas results by integrating pleiotropy and annotation. *PLoS Genetics*, 10(11):e1004787, 2014.

G. A. Churchill. Hidden markov chains and the analysis of genome structure. *Computers & Chemistry*, 16(2):107–115, 1992.

K. M. De Lange, L. Moutsianas, J. C. Lee, C. A. Lamb, Y. Luo, N. A. Kennedy, L. Jostins, D. L. Rice, J. Gutierrez-Achury, S.-G. Ji, et al. Genome-wide association study implicates immune activation of multiple integrin genes in inflammatory bowel disease. *Nature Genetics*, 49(2):256–261, 2017.

F. Demenais, P. Margaritte-Jeannin, K. C. Barnes, W. O. Cookson, J. Altmüller, W. Ang, R. G. Barr, T. H. Beaty, A. B. Becker, J. Beilby, et al. Multiancestry association study identifies new asthma risk loci that colocalize with immune-cell enhancer marks. *Nature Genetics*, 50(1):42–53, 2018.

A. P. Dempster, N. M. Laird, and D. B. Rubin. Maximum likelihood from incomplete data via the em algorithm. *Journal of the Royal Statistical Society: Series B (Methodological)*, 39(1):1–22, 1977.

R. Durrett. *Probability: theory and examples*. Cambridge university press, 2019.

B. Efron. *Large-scale inference: empirical Bayes methods for estimation, testing, and prediction*. Cambridge University Press, 2012.

medRxiv preprint doi: https://doi.org/10.1101/2023.09.04.23295018; this version posted September 5, 2023. The copyright holder for this preprint (which was not certified by peer review) is the author/funder, who has granted medRxiv a license to display the preprint in perpetuity. All rights reserved. No reuse allowed without permission.

M. A. Ferreira, M. C. Matheson, C. S. Tang, R. Granell, W. Ang, J. Hui, A. K. Kiefer, D. L. Duffy, S. Baltic, P. Danoy, et al. Genome-wide association analysis identifies 11 risk variants associated with the asthma with hay fever phenotype. *Journal of Allergy and Clinical Immunology*, 133(6):1564–1571, 2014.

M. A. Ferreira, J. M. Vonk, H. Baurecht, I. Marenholz, C. Tian, J. D. Hoffman, Q. Helmer, A. Tillander, V. Ullemar, J. Van Dongen, et al. Shared genetic origin of asthma, hay fever and eczema elucidates allergic disease biology. *Nature Genetics*, 49(12):1752–1757, 2017.

L. P. Freedman, I. M. Cockburn, and T. S. Simcoe. The economics of reproducibility in preclinical research. *PLoS Biology*, 13(6):e1002165, 2015.

R. Heller and D. Yekutieli. Replicability analysis analysis for genome-wide association studies. *Annals of Applied Statistics*, 8(1):481–498, 2014.

R. Heller, S. Yaacoby, and D. Yekutieli. repfdr: a tool for replicability analysis for genome-wide association studies. *Bioinformatics*, 30(20):2971–2972, 2014.

J. Huffman. Examining the current standards for genetic discovery and replication in the era of mega-biobanks. *Nature Communications*, 9(1):5054, 2018.

J. Ioannidis, E. E. Ntzani, T. A. Trikalinos, and D. G. Contopoulos-Ioannidis. Replication validity of genetic association studies. *Nature Genetics*, 29(3):306–309, 2001.

J. P. Ioannidis. Why most published research findings are false. *PLoS Medicine*, 2(8):e124, 2005.

T. Lappalainen, M. Sammeth, M. R. Friedländer, P. A. 't Hoen, J. Monlong, M. A. Rivas, M. Gonzalez-Porta, N. Kurbatova, T. Griebel, P. G. Ferreira, et al. Transcriptome and genome sequencing uncovers functional variation in humans. *Nature*, 501(7468):506–511, 2013.

medRxiv preprint doi: https://doi.org/10.1101/2023.09.04.23295018; this version posted September 5, 2023. The copyright holder for this preprint (which was not certified by peer review) is the author/funder, who has granted medRxiv a license to display the preprint in perpetuity. All rights reserved. No reuse allowed without permission.

N. Li and M. Stephens. Modeling linkage disequilibrium and identifying recombination hotspots using single-nucleotide polymorphism data. *Genetics*, 165(4):2213–2233, 2003.

Q. Li, J. B. Brown, H. Huang, and P. J. Bickel. Measuring reproducibility of high-throughput experiments. *Annals of Applied Statistics*, 5(3):1752–1779, 2011.

Y. Li, X. Zhou, R. Chen, X. Zhang, and H. Cao. Stareg: an empirical bayesian approach to detect replicable spatially variable genes in spatial transcriptomic studies. *bioRxiv*, 2023.

J. Z. Liu, S. Van Sommeren, H. Huang, S. C. Ng, R. Alberts, A. Takahashi, S. Ripke, J. C. Lee, L. Jostins, T. Shah, et al. Association analyses identify 38 susceptibility loci for inflammatory bowel disease and highlight shared genetic risk across populations. *Nature Genetics*, 47(9):979–986, 2015.

C. Lonjou, W. Zhang, A. Collins, W. J. Tapper, E. Elahi, N. Maniatis, and N. E. Morton. Linkage disequilibrium in human populations. *Proceedings of the National Academy of Sciences*, 100(10):6069–6074, 2003.

J. MacArthur, E. Bowler, M. Cerezo, L. Gil, P. Hall, E. Hastings, H. Junkins, A. McMahon, A. Milano, J. Morales, et al. The new nhgri-ebi catalog of published genome-wide association studies (gwas catalog). *Nucleic Acids Research*, 45(D1):D896–D901, 2017.

M. I. McCarthy, G. R. Abecasis, L. R. Cardon, D. B. Goldstein, J. Little, J. P. Ioannidis, and J. N. Hirschhorn. Genome-wide association studies for complex traits: consensus, uncertainty and challenges. *Nature Reviews Genetics*, 9(5):356–369, 2008.

D. McGuire, Y. Jiang, M. Liu, J. D. Weissenkampen, S. Eckert, L. Yang, F. Chen, A. Berg, S. Vrieze, et al. Model-based assessment of replicability for genome-wide association meta-analysis. *Nature Communications*, 12(1):1964, 2021.

medRxiv preprint doi: https://doi.org/10.1101/2023.09.04.23295018; this version posted September 5, 2023. The copyright holder for this preprint (which was not certified by peer review) is the author/funder, who has granted medRxiv a license to display the preprint in perpetuity. All rights reserved. No reuse allowed without permission.

N. A. Molodecky, S. Soon, D. M. Rabi, W. A. Ghali, M. Ferris, G. Chernoff, E. I. Benchimol, R. Panaccione, S. Ghosh, H. W. Barkema, et al. Increasing incidence and prevalence of the inflammatory bowel diseases with time, based on systematic review. *Gastroenterology*, 142 (1):46–54, 2012.

R. Moonesinghe, M. J. Khoury, T. Liu, and J. P. Ioannidis. Required sample size and non-replicability thresholds for heterogeneous genetic associations. *Proceedings of the National Academy of Sciences*, 105(2):617–622, 2008.

K. P. Murphy. *Machine learning: a probabilistic perspective*. MIT press, 2012.

J. K. Nowak, A. Glapa-Nowak, A. Banaszkiewicz, B. Iwańczak, J. Kwiecień, A. Szaflarska-Popławska, U. Grzybowska-Chlebowczyk, M. Osiecki, J. Kierkuś, M. Hołubiec, et al. Hla-dqa1* 05 associates with extensive ulcerative colitis at diagnosis: An observational study in children. *Genes*, 12(12):1934, 2021.

T. A. Olafsdottir, F. Theodors, K. Bjarnadottir, U. S. Bjornsdottir, A. B. Agustsdottir, O. A. Stefansson, E. V. Ivarsdottir, J. K. Sigurdsson, S. Benonisdottir, G. I. Eyjolfsson, et al. Eighty-eight variants highlight the role of t cell regulation and airway remodeling in asthma pathogenesis. *Nature Communications*, 11(1):393, 2020.

D. Philtron, Y. Lyu, Q. Li, and D. Ghosh. Maximum rank reproducibility: a nonparametric approach to assessing reproducibility in replicate experiments. *Journal of the American Statistical Association*, 113(523):1028–1039, 2018.

J. Piñero, À. Bravo, N. Queralt-Rosinach, A. Gutiérrez-Sacristán, J. Deu-Pons, E. Centeno, J. García-García, F. Sanz, and L. I. Furlong. Disgenet: a comprehensive platform integrating information on human disease-associated genes and variants. *Nucleic Acids Research*, 2015: gkw943, 2015.

medRxiv preprint doi: https://doi.org/10.1101/2023.09.04.23295018; this version posted September 5, 2023. The copyright holder for this preprint (which was not certified by peer review) is the author/funder, who has granted medRxiv a license to display the preprint in perpetuity. All rights reserved. No reuse allowed without permission.

F. Prinz, T. Schlange, and K. Asadullah. Believe it or not: how much can we rely on published data on potential drug targets? *Nature Reviews Drug Discovery*, 10(9):712–712, 2011.

J. K. Pritchard and M. Przeworski. Linkage disequilibrium in humans: models and data. *American Journal of Human Genetics*, 69(1):1–14, 2001.

L. Rabiner and B. Juang. An introduction to hidden markov models. *IEEE ASSP Magazine*, 3(1):4–16, 1986.

M. Reinshagen, C. Loeliger, P. Kuehnl, U. Weiss, B. Manfras, G. Adler, and B. Boehm. Hla class ii gene frequencies in crohn's disease: a population based analysis in germany. *Gut*, 38(4):538–542, 1996.

T. Robertson, R. L. Dykstra, and F. T. Wright. Order restricted statistical inference. In *Wiley Series in Probability and Mathematical Statistics*. John Wiley and Sons, 1988.

A. D. Skol, L. J. Scott, G. R. Abecasis, and M. Boehnke. Joint analysis is more efficient than replication-based analysis for two-stage genome-wide association studies. *Nature Genetics*, 38(2):209–213, 2006.

C. Sudlow, J. Gallacher, N. Allen, V. Beral, P. Burton, J. Danesh, P. Downey, P. Elliott, J. Green, M. Landray, et al. Uk biobank: an open access resource for identifying the causes of a wide range of complex diseases of middle and old age. *PLoS Medicine*, 12(3):e1001779, 2015.

W. Sun and T. Cai. Large-scale multiple testing under dependence. *Journal of the Royal Statistical Society: Series B (Statistical Methodology)*, 71(2):393–424, 2009.

W. Sun and T. T. Cai. Oracle and adaptive compound decision rules for false discovery rate control. *Journal of the American Statistical Association*, 102(479):901–912, 2007.

medRxiv preprint doi: https://doi.org/10.1101/2023.09.04.23295018; this version posted September 5, 2023. The copyright holder for this preprint (which was not certified by peer review) is the author/funder, who has granted medRxiv a license to display the preprint in perpetuity. All rights reserved. No reuse allowed without permission.

494 J. D. Wall and J. K. Pritchard. Haplotype blocks and linkage disequilibrium in the human
495 genome. *Nature Reviews Genetics*, 4(8):587–597, 2003.

496 G. Wang, A. Sarkar, P. Carbonetto, and M. Stephens. A simple new approach to variable
497 selection in regression, with application to genetic fine mapping. *Journal of the Royal*
498 *Statistical Society Series B: Statistical Methodology*, 82(5):1273–1300, 2020.

499 Z. Wei, W. Sun, K. Wang, and H. Hakonarson. Multiple testing in genome-wide association
500 studies via hidden markov models. *Bioinformatics*, 25(21):2802–2808, 2009.

501 D. Welter, J. MacArthur, J. Morales, T. Burdett, P. Hall, H. Junkins, A. Klemm, P. Flicek,
502 T. Manolio, L. Hindorff, et al. The nhgri gwas catalog, a curated resource of snp-trait
503 associations. *Nucleic Acids Research*, 42(D1):D1001–D1006, 2014.

504 X. Wen, Y. Lee, F. Luca, and R. Pique-Regi. Efficient integrative multi-snp association
505 analysis via deterministic approximation of posteriors. *The American Journal of Human*
506 *Genetics*, 98(6):1114–1129, 2016.

507 Y. Zhao, M. G. Sampson, and X. Wen. Quantify and control reproducibility in high-
508 throughput experiments. *Nature Methods*, 17(12):1207–1213, 2020.

509 Z. Zhu, P. H. Lee, M. D. Chaffin, W. Chung, P.-R. Loh, Q. Lu, D. C. Christiani, and L. Liang.
510 A genome-wide cross-trait analysis from uk biobank highlights the shared genetic architec-
511 ture of asthma and allergic diseases. *Nature Genetics*, 50(6):857–864, 2018.

512 Z. Zhu, Y. Guo, H. Shi, C.-L. Liu, R. A. Panganiban, W. Chung, L. J. O'Connor, B. E. Himes,
513 S. Gazal, K. Hasegawa, et al. Shared genetic and experimental links between obesity-related
514 traits and asthma subtypes in uk biobank. *Journal of Allergy and Clinical Immunology*,
515 145(2):537–549, 2020.